

RESEARCH ARTICLE

Open Access



α -synuclein-lanthanide metal ions interaction: binding sites, conformation and fibrillation

Jia Bai^{1,2}, Zeting Zhang¹, Maili Liu¹ and Conggang Li^{1*}

Abstract

Background: The pathological hallmark of Parkinson's disease is the deposition of cytoplasmic neuronal inclusions termed Lewy bodies. The major component of Lewy bodies is amyloid fibrils of α -synuclein. To investigate what causes α -synuclein aggregation is essential to understand its pathological roles in Parkinson's disease. Various metal ions, including iron and copper, have been implicated in the pathogenesis of Parkinson's disease. Divalent metal ions can regulate α -synuclein fibrillation rate, however, few studies have been performed to investigate how trivalent metal ions interact with α -synuclein and their effect on α -synuclein fibrillation. The study of the interaction between divalent and trivalent metal ions with α -synuclein is of vital importance to realize the mechanism of α -synuclein fibrillation.

Results: Here we used nuclear magnetic resonance spectroscopy to determine the trivalent metal ions (lanthanides) binding sites in α -synuclein. We found that lanthanide metal ions not only bind non-specifically to the C-terminal domain of α -synuclein, but also transiently interact with residues contain carboxyl groups in the N-terminal and NAC regions, the latter binding sites were not found for divalent cations. In addition, lanthanide ions bound α -synuclein exhibits slower conformational exchange rate. Compare to divalent cations, lanthanide ions accelerate α -synuclein fibrillation much faster.

Conclusions: We identified the lanthanide metal ions binding sites in α -synuclein and found a hierarchal effect for lanthanide ions binding to α -synuclein, driven by the interaction with aspartic acids and glutamic acids residues. Lanthanide ions binding also induced conformational dynamics change of α -synuclein. Compared to divalent cations, lanthanide metal ions significantly accelerated α -synuclein fibrillation, possibly due to the different inherent properties such as charge, binding sites and coordination modes.

Keywords: α -synuclein (α S), Lanthanide metal ions, Binding sites, Fibrillation

Background

Parkinson's disease (PD) is a common neurodegenerative disease of the population over 65 [1]. The histological hallmark of Parkinson's disease is the selective missing of dopaminergic neurons in the substantia nigra pars compacta. Intraneuronal deposits of fibrillar and misfolded proteins called the Lewy bodies appear in the affected brain areas.

The main component of the Lewy bodies is α -synuclein (α S) aggregates [1–3]. Investigating what causes α S aggregation is important to understand its pathological roles in PD.

In aqueous solution, monomeric α S is a natively unfolded protein with no apparent ordered secondary structure detectable by Far-UV Circular Dichroism (CD), Fourier transform infrared spectroscopy, or nuclear magnetic resonance (NMR) spectroscopy [4–6], but it forms β -sheet riched amyloid like fibrils under certain conditions [4, 7–9]. The N-terminal of α S exhibits a partially α -helical secondary structure upon binding with negatively phospholipid membranes and detergent micelles, while the C-terminus still remains dynamically unstructured [10–14]. α S has 140 amino acids with three

* Correspondence: conggangli@wipm.ac.cn

¹Key Laboratory of Magnetic Resonance in Biological Systems, State Key Laboratory of Magnetic Resonance and Atomic and Molecular Physics, National Center of Magnetic Resonance in Wuhan, Wuhan Institute of Physics and Mathematics, Chinese Academy of Sciences, Wuhan 430071, P.R. China

Full list of author information is available at the end of the article



distinct regions: the positively charged N-terminal region (residues 1–60); the hydrophobic NAC (non-amyloid β component) region (residues 61–95); and the highly negatively charged C-terminal region (residues 96–140) [15, 16]. The exposure of NAC region is considered as the main reason for α S fibrillation [16]. α S has the structural properties of auto-inhibition fibrillation due to the long-range transient intra-molecular interaction between the N-terminus and the C-terminus, which protecting NAC region from exposure [17–20].

Increasing evidences have shown that altered metal homeostasis might be involved in the progression of neurodegenerative diseases. The possible involvement of heavy metals in the etiology of PD followed primarily from the results of epidemiological studies [21–24] and Lewy bodies component analysis in the parkinsonian substantia nigra [25, 26]. The potential link between metal ions and the PD related protein α S was observed in *in vitro* experiments. Recent studies show that the binding affinities of α S for diverse metal ions are different, but the binding sites are similar for the majority of metal ions. For divalent cations such as Fe^{2+} , Mn^{2+} , Co^{2+} , Ni^{2+} and Ca^{2+} , they all bound non-specifically to the C-terminal domain of α S [27–29]. But for Cu^{2+} , it has high affinity to the α S N-terminus, and low affinity to the C-terminus [27, 30, 31]. No conformational change of α S was observed at low ionic concentration of various ions. At high concentration of metal ions, K^+ , Na^+ , Li^+ , Cs^+ , and Ca^{2+} has no effect on the unfolded structure of α S, but Mn^{2+} , Cd^{2+} , Mg^{2+} and Zn^{2+} induce a small increase in α -helix contents, and Cu^{2+} , Co^{2+} , Fe^{3+} and Al^{3+} induce more α -helix contents [32, 33].

Recently, studies have shown that lanthanide ions might affect the neuronal systems, but the toxicological behaviours were very complicated and the effects depended on a variety of factors [34–36]. With the increasing applications of lanthanides in industry, agriculture and medicine [37–41], particularly for the people who has long-term exposure in the electronics components industry or mining, public concern pays more and more attention on the toxicity of the lanthanides. In this study, we characterized the interaction between lanthanide metal ions (Ln^{3+}) with recombinant human α S and the binding sites (region) were determined using NMR spectroscopy. We found that lanthanide metal ions accelerated α S fibrillation much faster than divalent cations *in vitro*. Based on the interaction information, we proposed the mechanism by which lanthanide metal ions accelerated α S fibrillation *in vitro*.

Results and discussion

Lanthanide metal ions binding sites determination

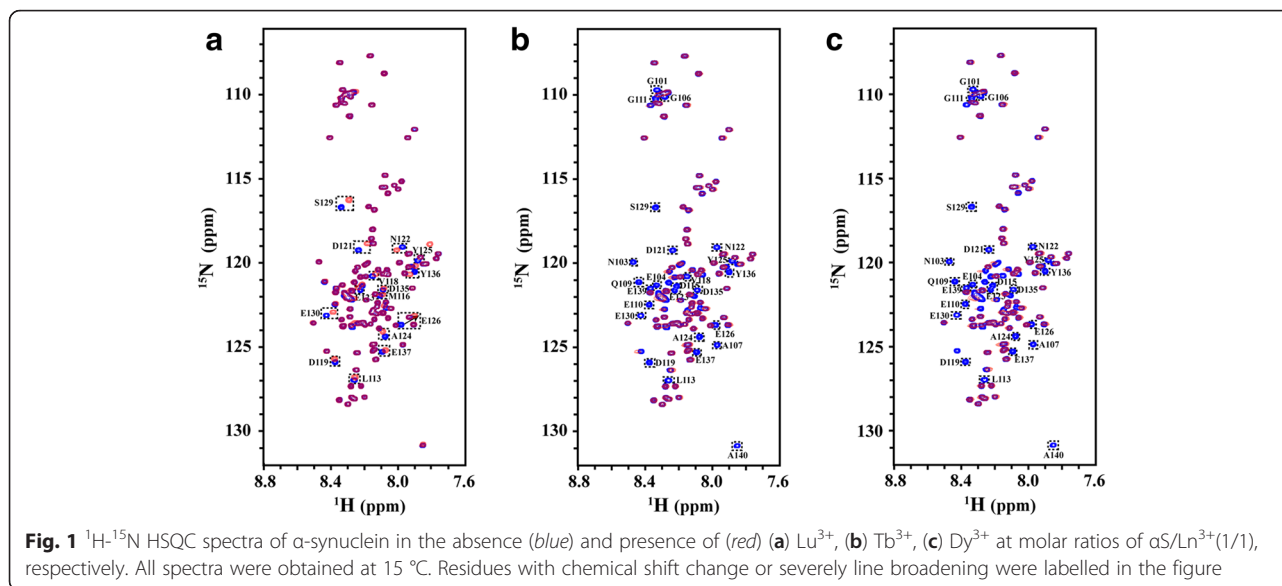
The ^1H - ^{15}N heteronuclear single quantum correlation (HSQC) spectrum that contains one cross peak for each

amide group (except proline) in a protein is routinely used to characterize protein-ligand and protein-protein interactions. The lanthanide metal ions (Ln^{3+}) binding sites in α S were identified by using chemical shift perturbation of ^1H - ^{15}N HSQC NMR spectroscopy of α S in the absence and presence of Ln^{3+} at various concentration ratios. We collected a series of ^1H - ^{15}N HSQC spectra of α S from 0 to 1/4 molar ratio of $\alpha\text{S}/\text{Ln}^{3+}$. Fig. 1 showed ^1H - ^{15}N HSQC spectra of α S in the absence (blue) and presence (red) of Ln^{3+} at 1/1 molar ratio of $\alpha\text{S}/\text{Ln}^{3+}$, respectively. In the presence of diamagnetic Lu^{3+} , the residues with significant chemical shift changes were labelled in Fig. 1a, and the assignments were according to Biological Magnetic Resonance Data Bank (BMRB entry number is 16,543 for α -synuclein). In the presence of paramagnetic Tb^{3+} and Dy^{3+} , the cross peaks of some residues became severely broadening and disappeared (Fig. 1b and c) due to paramagnetic relaxation enhancement effects, these residues were similar as those showing chemical shift changes in Fig. 1a. The ^1H - ^{15}N spectra of α S in the presence of Ln^{3+} were also characteristic spectra of unfolded protein, suggesting that binding with Ln^{3+} might not cause significant structural change of α S.

To map the binding sites of Lu^{3+} in α S, the chemical shift perturbations $\Delta\delta_{\text{N-H}}$ induced by Lu^{3+} were plotted as a function of α S sequence. As shown in Fig. 2, significant chemical shift perturbations were located from residue 110 to 140 in the C-terminal region and residue Y125 with the largest chemical shift perturbation, whereas small or no change was observed for the residues in the N-terminal and NAC regions. With the molar ratio of $\alpha\text{S}/\text{Ln}^{3+}$ decreased from 4/1 to 1/1, the chemical shift perturbation of residues at the C-terminal region became larger, suggesting that Lu^{3+} binding with α S in the C-terminal region centered at residue Y125.

The intensity ratios of cross peaks in the presence (I) and absence of Lu^{3+} (I_0) were also shown in Fig. 2d-f. When the molar ratio of $\text{Lu}^{3+}/\alpha\text{S}$ decreased from 4/1 to 1/1, the signal intensity of residues located in the C-terminal region decreased, whereas small or no change was observed for the residues in the N-terminal and NAC regions. We also noticed that many cross peaks of C-terminal residues disappear when $\alpha\text{S}/\text{Lu}^{3+}$ ratio decreased further to 1/10 (Additional file 1: Figure S1), suggesting that binding with Lu^{3+} slows down α S conformational exchange rate.

In contrast to diamagnetic Lu^{3+} , we did not observe residues with significant chemical shift change in the presence of the paramagnetic ions (Tb^{3+} , Dy^{3+}). By analysing the ^1H - ^{15}N HSQC spectra, we found that some cross peaks showed significant intensity decrease and some cross peaks were even too broad to detect as a result of paramagnetic effects of Tb^{3+} and Dy^{3+} . We plot

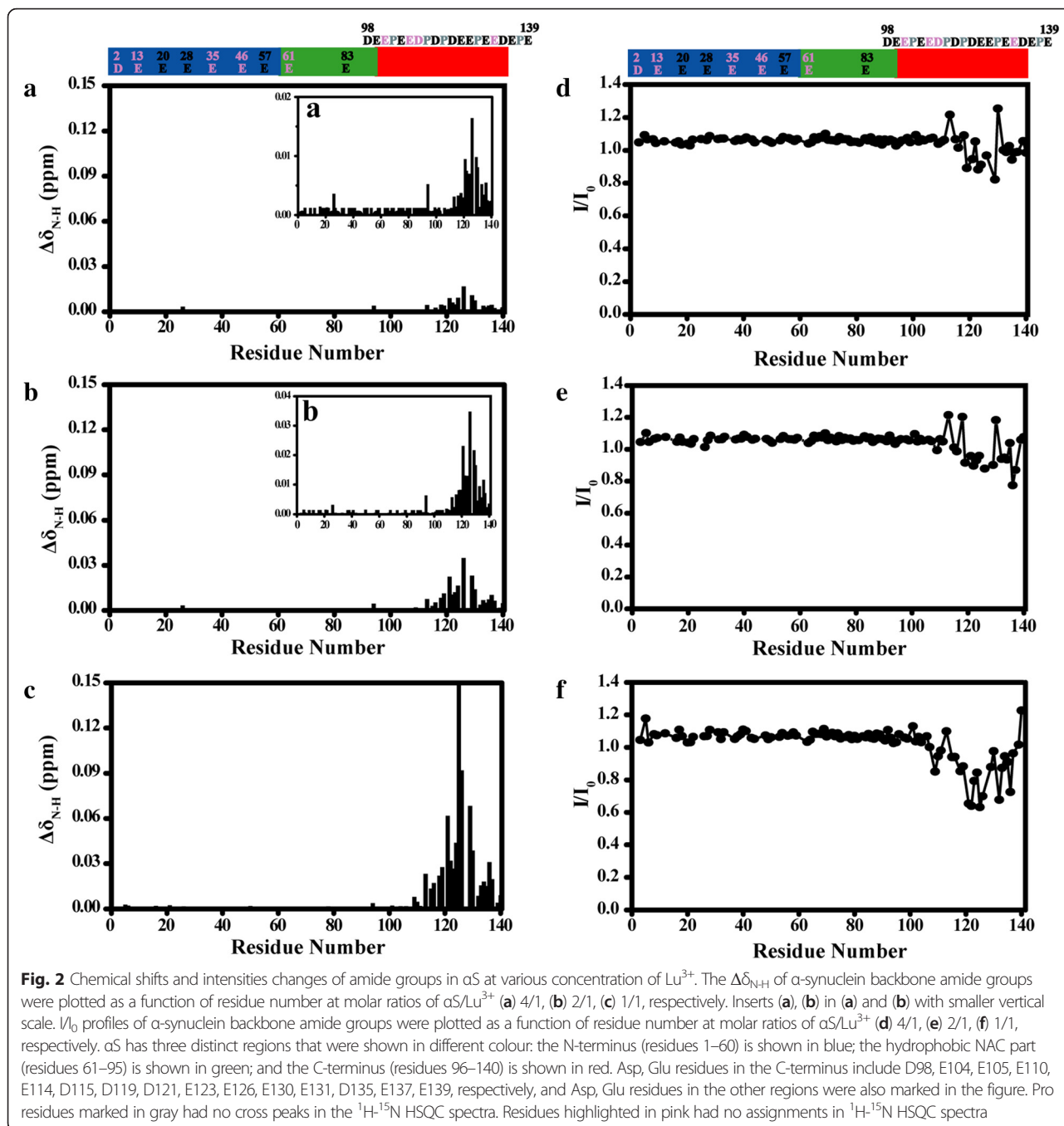


the intensity ratios (I/I_0) of cross peaks in the presence (I) and absence of Tb^{3+} (or Dy^{3+}) (I_0) as a function of αS sequence. As shown in Fig. 3, the intensity of C-terminal residues decreased much more than that of residues in the N-terminal and NAC region. A comparative analysis with Tb^{3+} and Dy^{3+} revealed a hierarchy in the binding of lanthanide ions to αS . According to the attenuation profile of cross peaks (I/I_0), the whole residues of αS were divided into three parts: residues 1 to 97, residues 98 to 109, and residues 110 to 140. It is clear that the lanthanide ions bound preferentially to the region comprising residues 110–140, the secondary binding regions may contain residues 98–109, and the weak interaction binding regions contained residues in 1–97 regions, which were labelled with orange lines in Fig. 3. With the molar ratio of $\alpha\text{S}/\text{Ln}^{3+}$ decreased from 4/1 to 1/1, the I/I_0 values of all the residues other than the residues in the C-terminal region decreased, while the I/I_0 values of residues 3, 20, 21, 28, 57, 58, 59, 83, 84 decreased more than other residues in the N-terminal and NAC regions. We found these residues are aspartic acid and glutamic acid residues or residues near to aspartic acid and glutamic acid (Fig. 3). Interestingly, they are all negatively charged residues that have a carboxyl groups in the side-chain, which may have transient weak interactions with positively charged lanthanide ions. αS C-terminus contains many aspartic acid and glutamic acid residues and it was reasonable that lanthanide ions bound preferentially to this region.

We also used ^1D ^1H spectra to obtain information on the roles of αS aromatic side chains in lanthanide binding. The ^1H NMR spectra of αS in D_2O (6.3–7.5 ppm) comprised the side chains of different aromatic residues: Phe (F4, F94), Tyr (Y39, Y125, Y133, Y136) (Additional file 1: Figure S2 and Figure S3), and the signals were assigned

according to previous reports [27]. In the presence of low concentration lanthanide ions (Tb^{3+} and Dy^{3+}), the Tyr signals intensity decrease significant, and with lanthanide ions (Tb^{3+} and Dy^{3+}) concentration increasing, the Phe signals were further affected, suggesting lanthanide ions bound preferentially to C-terminus and might have transient weak interactions with N-terminal and NAC regions, consistent with ^1H - ^{15}N HSQC spectra.

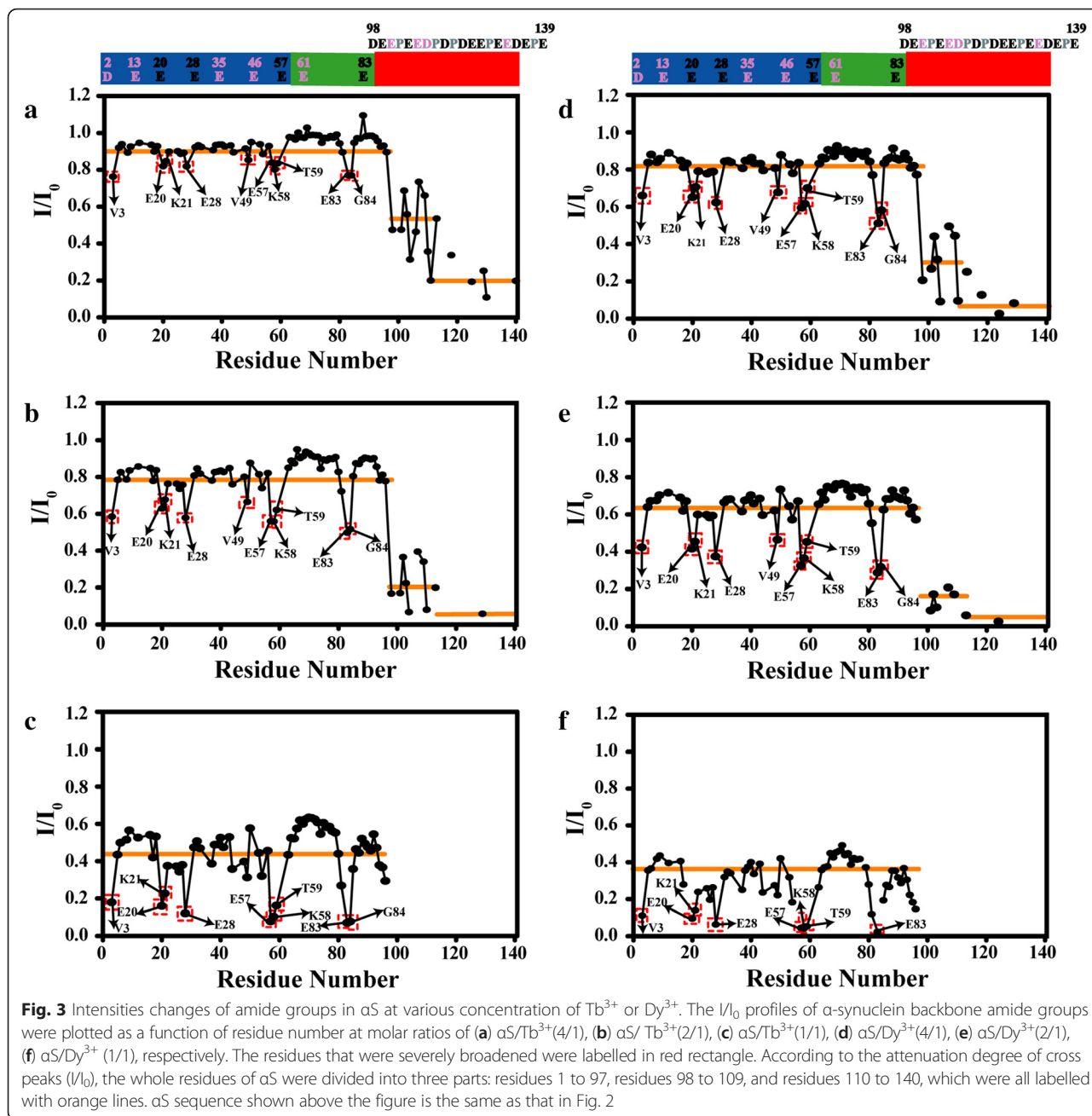
Many other metal ions and polyamines [42] also bind to the αS C-terminal region from residue 110 to 140. Other than the C-terminus, weaker binding sites involved residues 46–55 in the αS N-terminus was also reported for paramagnetic divalent cations such as Fe^{2+} and Co^{2+} [27]. For Cu^{2+} , the specific binding sites were identified as residues Met1, Asp2, and His50 in the N-terminus [27, 30]. It was worth mentioning that the binding sites of Ln^{3+} involved residues different from those binding with other divalent cations [27, 28, 30]. Residues containing a carboxyl groups in the N-terminal and NAC regions also have transient weak interaction with lanthanide ions. The binding character difference might be due to the inherent properties of different metal ions, such as charge, ionic radii and coordination abilities. The lanthanide metal ions, which possess ionic radii similar to Ca^{2+} , are assumed to behave very similar to Ca^{2+} in protein binding. Through NMR titration experiment, we found that Ca^{2+} binding sites located in the αS C-terminus (Additional file 1: Figure S4 and Figure S5). The chemical shift perturbations of C-terminal residues are much smaller in the presence of Ca^{2+} than that of Lu^{3+} , suggesting that αS - Ca^{2+} binding is relatively weak. The pattern of the chemical shift perturbation was also different from that induced by lanthanides ions. Our observations suggest that although



lanthanides ions have similar ionic radii to Ca^{2+} , they show different binding properties with α S. Diamagnetic metal ion Al^{3+} was also reported as an effective promoter to α S fibrillation, and we also studied Al^{3+} binding sites in α S (Additional file 1: Figure S6 and Figure S7). We found no obvious chemical shift perturbations were observed in the presence of Al^{3+} , and only large intensity attenuation of cross peaks were located in the α S C-terminus, which suggested that binding with Al^{3+} slows down α S conformational exchange rate. Such conformational

exchange was also observed in the presence of high concentration of Lu^{3+} (Additional file 1: Figure S1).

Since the affinities for the Ln^{3+} with α S is similar, the different degree of broadening for Dy^{3+} and Tb^{3+} must be from slightly different paramagnetic properties: the total angular momentum quantum number J for Dy^{3+} is 15/2, which is a little larger than that for Tb^{3+} ($J = 6$), meanwhile the unpaired electron correlation time τ_e of Dy^{3+} is $0.3 \times 10^{-12}\text{s}$, which is a little larger than that of Tb^{3+} ($\tau_e = 0.2 \times 10^{-12}\text{s}$) [43]. These different properties

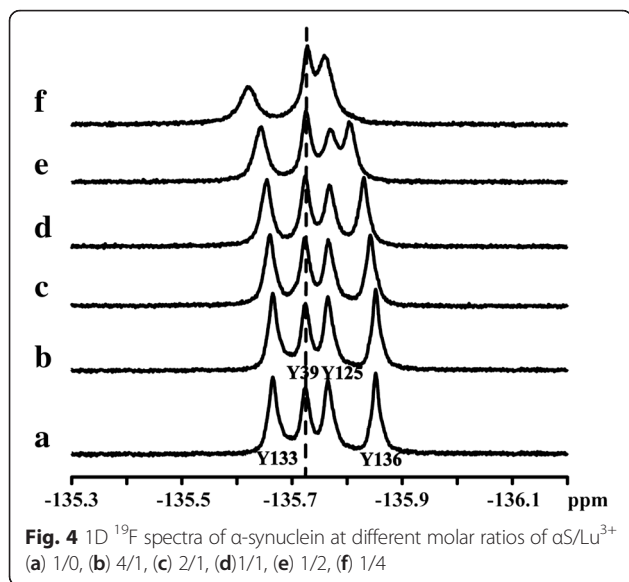


may explain why the intensity ratios of cross peaks in the presence of Dy^{3+} decrease more severely than that in the presence of Tb^{3+} . The strong paramagnetic properties of lanthanide ions might have solvent PRE effect, which makes the cross peaks intensity ratios of most observed residues in the N-terminal and NAC region decreased to 0.4 or 0.6 (Fig. 3c, f).

As for diamagnetic ion (Lu^{3+}), significant chemical shift perturbations were not observed in the N-terminal and NAC regions. It may be due to the fact that PRE is more sensitive to local structural perturbation than chemical shift, because paramagnetic relaxation enhancement is

proportional to r^{-6} , where r is the distance between paramagnetic ion and nucleus observed.

To further confirm the binding sites, ^{19}F NMR was also employed to study the α S - Lu^{3+} interaction. The ^{19}F chemical shift is sensitive to the change of local chemical environment, hence it is a good reporter of binding sites. $3-^{19}F$ tyrosine labelled α S were prepared and 1D ^{19}F NMR spectra were recorded at different concentration ratios of Lu^{3+} (Fig. 4). The four ^{19}F resonances (tyrosine 133, 39, 125, 136) were assigned according to previous research [44]. From Fig. 4, the ^{19}F chemical shift of residue 39 in the N-terminus remained the same at different α S/ Lu^{3+}

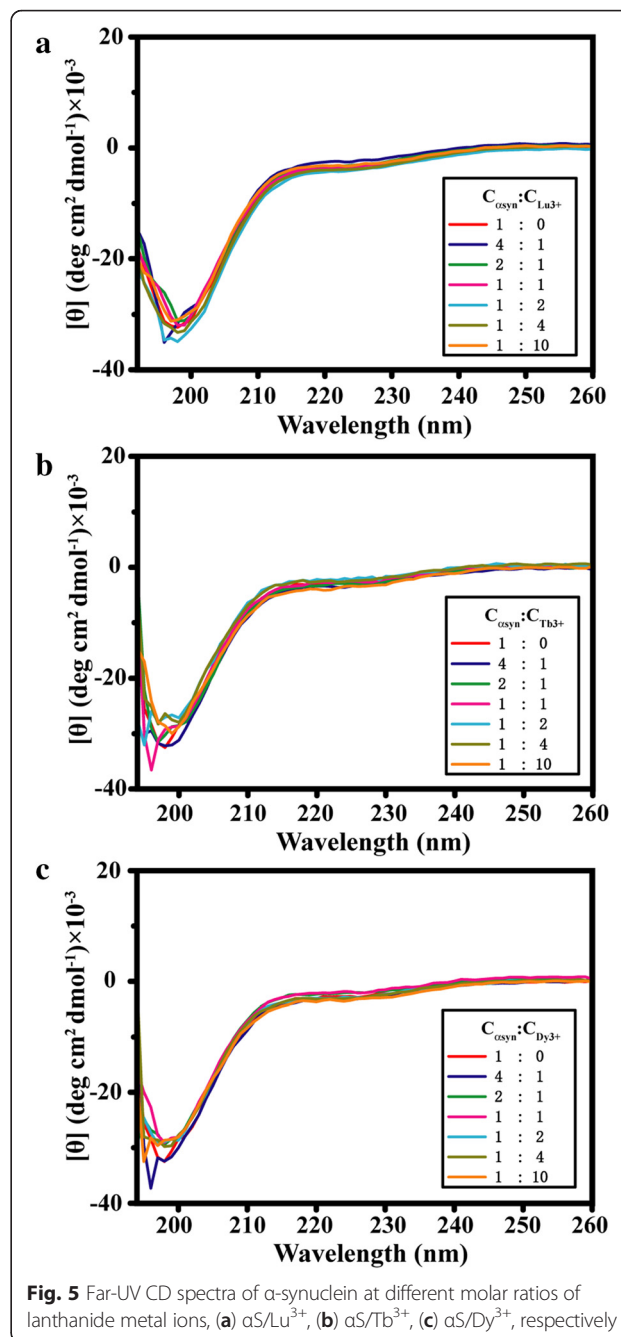


ratios, however, chemical shift and shape of residues 125, 133, 136 in the C-terminal region changed during the titrations, indicating the binding is in the fast time scale and is weak as the titration is incomplete. The results suggested that the primary binding sites of Lu³⁺ located at C-terminal region, which was consistent with ¹H-¹⁵N HSQC and 1D ¹H experimental results. In a word, like many divalent metal ions such as Fe²⁺, Mn²⁺, Co²⁺, Ni²⁺ and Ca²⁺ [27, 28], lanthanide ions also bound non-specifically to the C-terminal domain of αS, and residues contain the carboxyl groups in the N-terminal and NAC regions that also have transient weak interaction with lanthanide ions, which was not reported in other studies of divalent metal ions interacting with αS.

Lanthanide metal ions effects on αS conformation

The narrow dispersion (7.8-8.3 ppm) of amide ¹H chemical shift suggested that αS remained disordered in the presence of lanthanide metal ions. Besides NMR spectroscopy, far-UV circular dichroism (CD) was also used to monitor the conformational change in presence of lanthanide metal ions. In the absence of Ln³⁺, the spectra of αS exhibited substantially disordered structure (no characteristic α-helix or β-sheet peaks in the 210–230 nm or 198 nm regions). In the presence of different ionic ratios, even in the higher ionic ratios, the spectra were always indicative of essentially unfolded protein, suggesting that lanthanide metal ions binding could not cause significant structural change of αS (Fig. 5).

The hydrodynamic property of a macromolecule has been extensively used to study conformational changes accompanying molecular unfolding, association and aggregation. We employed ¹H pulsed-field gradient NMR to investigate the hydrodynamic properties of the αS-Lu³⁺ complexes at different concentration ratios of



αS/Lu³⁺. We measured the hydrodynamic radiuses of αS in the absence and presence of Lu³⁺. The radius of αS in the free state was approximately 31 Å, consistent with previous reports [27], and no large changes were observed at different αS/Lu³⁺ concentration ratios (Table 1). It suggested that binding with Lu³⁺ did not affect αS size, or cause any inter-molecular association.

Lanthanide metal ions effects on αS fibrillation

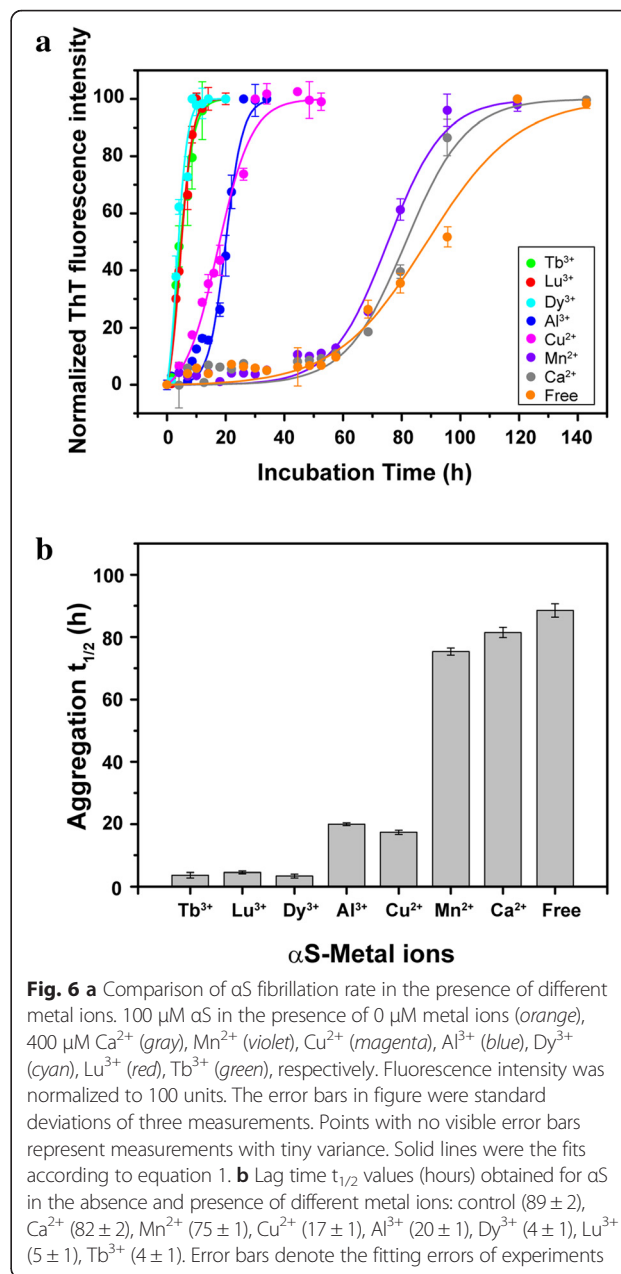
αS formed insoluble amyloid fibrils under some certain experimental conditions, and Thioflavin T (ThT) fluorescence

Table 1 The measured translational diffusion coefficients of dioxane and α -synuclein and the calculated hydrodynamic radius of α -synuclein at different concentration ratios of α S/Lu³⁺

$C_{\alpha S} : C_{Lu^{3+}}$	Translational diffusion coefficients		Hydrodynamic radius R_H (Å)
	α S (methyl regions from 0.87–0.56 ppm) $D_t \times 10^{-11}(\text{m}^2/\text{s})$	Dioxane (3.65–3.53 ppm) $D_t \times 10^{-10}(\text{m}^2/\text{s})$	
1 : 0	5.802 ± 0.001	8.482 ± 0.004	30.99 ± 0.05
4 : 1	5.949 ± 0.004	8.610 ± 0.004	30.68 ± 0.03
2 : 1	5.823 ± 0.006	8.488 ± 0.004	30.90 ± 0.04
1 : 1	5.845 ± 0.004	8.575 ± 0.004	31.10 ± 0.03
1 : 2	5.939 ± 0.003	8.626 ± 0.004	30.79 ± 0.02
1 : 4	5.915 ± 0.003	8.694 ± 0.005	31.16 ± 0.02

was generally used to monitor its fibrillation [45–48]. We studied α S fibrillation rates at different concentration ratios of α S to lanthanide metal ions (Additional file 1: Figure S8). The results indicated that α S fibrillation was accelerated in the presence of Ln³⁺, and the accelerating effect of Ln³⁺ depend on its concentration, higher concentration resulted in faster fibrillation. Different lanthanide metal ions seemed to have similar effects on promoting α S fibrillation. Compared to cations such as Al³⁺, Cu²⁺ and Mn²⁺, lanthanide metal ions (Lu³⁺, Dy³⁺, Tb³⁺) induced α S fibrillation much faster (Fig. 6). Ca²⁺, which possess ionic radii similar to lanthanide ions, are assumed to behave very similar to lanthanide ions in α S fibrillation, but to our surprise, Ca²⁺ did not significantly accelerate α S fibrillation. This result suggests that α S fibrillation kinetics can be modulated by interactions.

Many metal ions can accelerate α S fibrillation. The reason is very complex, and many factors involved in it. The different effects on α S fibrillation rate might be due to the inherent properties of different metal ions, such as binding sites, coordination modes. Positively charged metal ions neutralizing negatively charged α S, and resulting in stronger intermolecular association is also regarded as a reason for α S faster aggregation. Besides binding with α S C-terminus, lanthanide metal ions show very novel coordination modes, and residues contain the carboxyl groups in α S N-terminal and NAC regions that also have transient weak interaction with lanthanide ions, which is not reported in other studies of divalent metal ions interacting with α S. This specific interaction can disturb α S local conformation, and may be another reason for α S faster fibrillation. We also notice that many cross peaks of C-terminal residues disappear when α S/Lu³⁺ ratio decreased further to 1/10, suggesting that the presence of Lu³⁺ reduces the α S conformation exchange rate. Such conformational exchange reduction is also observed in the presence of Al³⁺. Slow α S conformational exchange rates make the expose hydrophobic residues contact long enough to form associated oligomers, which is crucial for protein fibrillation. When the



conformational exchange rate is fast or almost the same as the bimolecular encounter rate, there is not enough time for molecules association occurring.

Conclusions

In summary, we identified the lanthanide metal ions binding sites in α S by employing the chemical shift perturbations and paramagnetic effects of these metal ions. In particular, we found a hierarchal effect for lanthanide ions binding to α S, driven by the interaction with specific residues, namely, aspartic acids, glutamic acids residues. Compared to divalent cations, lanthanide metal ions significantly accelerated α S fibrillation,

possibly due to their different inherent properties such as charge, binding sites and coordination modes. The study here also suggest that binding induced change of conformational exchange dynamics provide a possible molecular mechanism to understanding α S fibrillation.

Methods

Protein expression and purification

Plasmids contained the coding sequence of α -synuclein were transformed into *Escherichia coli* strain BL21 (DE3) competent cells. Expression and purification of ^{15}N -labeled wild-type or ^{19}F -labeled (Y39F, Y125F, Y133F, Y136F) α -synuclein were performed as previously described [44, 49, 50].

Chemical Reagents

Thioflavin T (ThT), $\text{TbCl}_3 \cdot 6\text{H}_2\text{O}$, $\text{DyCl}_3 \cdot 6\text{H}_2\text{O}$ and $\text{LuCl}_3 \cdot 6\text{H}_2\text{O}$ from Sigma or Alfa Aesar were used without further purification. All other chemicals were of analytical grade from Sinopharm Chemical Reagent Co. Ltd.

Circular dichroism (CD) measurements

Samples containing 20 μM α S with different concentration of lanthanide metal ions in 10 mM MES and 100 mM NaCl at pH 6.0 were used for CD measurements. CD spectra were recorded on a ChirascanTM CD spectrometer in 10 mm cells from 260-190 nm with a step size of 1 nm and a bandwidth of 1 nm.

Fluorescence measurements

Samples comprised of 100 μM α S with 400 μM different metal ions in 10 mM MES, 100 mM NaCl, 500 μM phenylmethanesulfonyl (pH 6.0) were used for fibrillation experiments. α S fibril formation was induced at 37 $^\circ\text{C}$ by agitation with 220 rpm in the shaker. During fibrillation, small aliquots (10 μl) were removed and mixed with 1 mL 25 μM ThT. The fluorescence intensities were measured to monitor α S fibrillation. Fluorescence emission spectra were recorded at 482 nm on a HORIBA Fluoromax-4 spectrometer.

The aggregation data was analysed using equation (1) [42], where $\alpha[t]$ denotes the values measured by ThT fluorescence experiments, k_{app} is the apparent fibrillation rate constant, and $t_{1/2}$ is the lag time to the transition midpoint in the process from monomer to aggregate.

$$\alpha[t] = (1 - e^{-k_{\text{app}}t}) / (1 + e^{-k_{\text{app}}(t - t_{1/2})}) \quad (1)$$

NMR Spectroscopy and Data Analysis

NMR Buffer contained 10 mM MES, 100 mM NaCl (pH 6.0). Protein was concentrated to 0.25 mM in 90 %

NMR Buffer and 10 % D_2O . ^1H - ^{15}N HSQC spectra and diffusion experiments were acquired on a Bruker 600 MHz spectrometer equipped with a triple-resonance cryoprobe at 288 K. The HSQC spectra were acquired with sweep widths of 7212 Hz (^1H) and 1581 Hz (^{15}N), 2048 \times 256 complex points, 4 scans per t_1 point, and a 1.5 s recycle delay. The spectral widths for the diffusion experiments were 9615 Hz, with 32 K complex points, 56 scans, and a 1 s recycle delay. ^1D ^{19}F NMR spectra were acquired on a Bruker 600 MHz spectrometer equipped with a $^{19}\text{F}/^1\text{H}/^{13}\text{C}/^{15}\text{N}$ cryoprobe. Spectra were recorded with a 11.3 kHz sweep width, 350 scans, 16 K complex points and a recycle delay of 2 s. Proton decoupling was applied to all ^1D ^{19}F NMR spectra. Chemical shifts are referenced to trifluorotoluene at -63.72 ppm. For analysis of the chemical shift perturbations ($\Delta\delta_{\text{N-H}}$) of ^1H and ^{15}N backbone resonances in the HSQC spectra, a weighted average chemical shift change were calculated according to the equation (2) [51], where $\Delta\delta_{\text{H}}$ and $\Delta\delta_{\text{N}}$ denoted the chemical shift difference in the presence and in the absence of Ln^{3+} in the ^1H dimension and ^{15}N dimension, respectively.

$$\Delta\delta_{\text{N-H}} = \sqrt{\frac{(\Delta\delta_{\text{H}})^2 + (0.2(\Delta\delta_{\text{N}}))^2}{2}} \quad (2)$$

For the ^1H pulsed-field gradient NMR experiments, we used 1,4-dioxane as an internal radius standard (2.12 \AA) and viscosity probe. Diffusion spectra were acquired using the stimulated echo experiment with 3-9-19 pulse module for water suppression (stebpgp1s19). 20 linearly spaced values of gradient strength were used in the range from 0.963 to 45.74 G/cm. The optimized diffusion (Δ) and gradient pulse times (δ) were 0.45 s and 3 ms, respectively. Decays rates had been extracted from the spectra for both the protein (D_{prot}) and the reference molecule (D_{ref}), and the measured translational diffusion coefficients were showed in Table 1. The regions 0.87–0.56 ppm were used to calculate α S hydrodynamic radius (R_{h}) according to the equation (3) [52], where $R_{\text{h}}^{\text{prot}}$ was the protein hydrodynamic radius and $R_{\text{h}}^{\text{ref}}$ was the radius of the reference molecule. Spectra were processed and analysed by Topspin [53], NMRPipe [54], and Sparky [55].

$$R_{\text{h}}^{\text{prot}} = \frac{D_{\text{ref}}}{D_{\text{prot}}} * R_{\text{h}}^{\text{ref}} \quad (3)$$

Availability of supporting data

All the supporting data are included as Additional file 1.

Additional file

Additional file 1: Figure S1. Chemical shifts and intensities changes of amide groups in α S at various concentration of Lu^{3+} . **Figure S2.** Tb^{3+} effects on $^1\text{D}^1\text{H}$ spectra of α S aromatic side chains. **Figure S3.** Dy^{3+} effects on $^1\text{D}^1\text{H}$ spectra of α S aromatic side chains. **Figure S4.** Ca^{2+} effects on α S $^1\text{H}^15\text{N}$ -HSQC spectra. **Figure S5.** Chemical shifts and intensities changes of amide groups in α S at various concentration of Ca^{2+} . **Figure S6.** Al^{3+} effects on α S $^1\text{H}^15\text{N}$ -HSQC spectra. **Figure S7.** Intensities changes of amide groups in α S at various concentration of Al^{3+} . **Figure S8.** Fibrillation of α -synuclein monitored by ThT fluorescence in the presence of different lanthanide metal ions. (DOC 1028 kb)

Abbreviations

α S: α -synuclein; PD: Parkinson's disease; NMR: Nuclear magnetic resonance; HSQC: Heteronuclear single quantum correlation; CD: Circular Dichroism; Ln^{3+} : Lanthanide metal ions; ThT: Thioflavin T; MES: 2-(*N*-morpholino) ethanesulfonic acid; R_h : Hydrodynamic radius.

Competing interests

The authors declare that they have no competing interests.

Authors' contributions

Conceived and designed the experiments: JB, ZZ, ML, CL. Performed the experiments: JB. Analyzed the data: JB, ZZ, ML, CL. Wrote the paper: JB, ZZ, ML, CL. All authors read and approved the final manuscript.

Acknowledgements

This work is supported by Ministry of Science and Technology of China grant 2013CB910200 (C.L.), the 1000 Young Talents Program (C.L.), National Natural Sciences Foundation of China grant 21173258 (C.L.) and 21221064 (M.L.).

Author details

¹Key Laboratory of Magnetic Resonance in Biological Systems, State Key Laboratory of Magnetic Resonance and Atomic and Molecular Physics, National Center of Magnetic Resonance in Wuhan, Wuhan Institute of Physics and Mathematics, Chinese Academy of Sciences, Wuhan 430071, P.R. China. ²University of Chinese Academy of Sciences, Beijing 100049, China.

Received: 11 October 2015 Accepted: 15 January 2016

Published online: 03 February 2016

References

- Goedert M. Alpha-synuclein and neurodegenerative diseases. *Nat Rev Neurosci.* 2001;2(7):492–501.
- Forno LS. Neuropathology of Parkinson's Disease. *J Neuropathol Exp Neurol.* 1996;55(3):259–72.
- Spillantini MG, Schmidt ML, Lee VMY, Trojanowski JQ, Jakes R, Goedert M. [alpha]-Synuclein in Lewy bodies. *Nature.* 1997;388(6645):839–40.
- Uversky VN, Li J, Fink AL. Evidence for a partially folded intermediate in alpha-synuclein fibril formation. *J Biol Chem.* 2001;276(14):10737–44.
- Weinreb PH, Zhen W, Poon AW, Conway KA, Lansbury Jr PT. NACP, a protein implicated in Alzheimer's disease and learning, is natively unfolded. *Biochemistry.* 1996;35(43):13709–15.
- Bussell Jr R, Eliezer D. Residual structure and dynamics in Parkinson's disease-associated mutants of alpha-synuclein. *J Biol Chem.* 2001;276(49):45996–6003.
- Fink AL. The aggregation and fibrillation of α -synuclein. *Acc Chem Res.* 2006;39(9):628–34.
- Necula M, Chirita CN, Kuret J. Rapid anionic micelle-mediated alpha-synuclein fibrillization in vitro. *J Biol Chem.* 2003;278(47):46674–80.
- Sprangers R, Kay LE. Quantitative dynamics and binding studies of the 20S proteasome by NMR. *Nature.* 2007;445(7128):618–22.
- Eliezer D, Kutluay E, Bussell Jr R, Browne G. Conformational properties of α -synuclein in its free and lipid-associated states I. *J Mol Biol.* 2001;307(4):1061–73.
- Ulmer TS, Bax A. Comparison of structure and dynamics of micelle-bound human alpha-synuclein and Parkinson disease variants. *J Biol Chem.* 2005;280(52):43179–87.
- Georgieva ER, Ramlall TF, Borbat PP, Freed JH, Eliezer D. Membrane-bound alpha-synuclein forms an extended helix: long-distance pulsed ESR measurements using vesicles, bicelles, and rodlike micelles. *J Am Chem Soc.* 2008;130(39):12856–7.
- Bartels T, Ahlstrom LS, Leftin A, Kamp F, Haass C, Brown MF, et al. The N-terminus of the intrinsically disordered protein α -synuclein triggers membrane binding and helix folding. *Biophys J.* 2010;99(7):2116–24.
- Lokappa SB, Suk JE, Balasubramanian A, Samanta S, Situ AJ, Ulmer TS. Sequence and membrane determinants of the random coil-helix transition of alpha-synuclein. *J Mol Biol.* 2014;426(10):2130–44.
- Uversky VN. Neuropathology, biochemistry, and biophysics of alpha-synuclein aggregation. *J Neurochem.* 2007;103(1):17–37.
- Cho M-K, Nodet G, Kim H-Y, Jensen MR, Bernado P, Fernandez CO, et al. Structural characterization of α -synuclein in an aggregation prone state. *Protein Sci.* 2009;18(9):1840–6.
- Bertoncini CW, Jung YS, Fernandez CO, Hoyer W, Griesinger C, Jovin TM, et al. Release of long-range tertiary interactions potentiates aggregation of natively unstructured alpha-synuclein. *Proc Natl Acad Sci U S A.* 2005;102(5):1430–5.
- Lee JC, Gray HB, Winkler JR. Tertiary contact formation in alpha-synuclein probed by electron transfer. *J Am Chem Soc.* 2005;127(47):16388–9.
- Lee JC, Langen R, Hummel PA, Gray HB, Winkler JR. Alpha-synuclein structures from fluorescence energy-transfer kinetics: implications for the role of the protein in Parkinson's disease. *Proc Natl Acad Sci U S A.* 2004;101(47):16466–71.
- Dedmond MM, Lindorff-Larsen K, Christodoulou J, Vendruscolo M, Dobson CM. Mapping long-range interactions in alpha-synuclein using spin-label NMR and ensemble molecular dynamics simulations. *J Am Chem Soc.* 2005;127(2):476–7.
- Rybicki BA, Johnson CC, Uman J, Gorell JM. Parkinson's disease mortality and the industrial use of heavy metals in Michigan. *Mov Disord.* 1993;8(1):87–92.
- Gorell JM, Johnson CC, Rybicki BA, Peterson EL, Kortsha GX, Brown GG, et al. Occupational exposures to metals as risk factors for Parkinson's disease. *Neurology.* 1997;48(3):650–8.
- Gorell JM, Johnson CC, Rybicki BA, Peterson EL, Kortsha GX, Brown GG, et al. Occupational exposure to manganese, copper, lead, iron, mercury and zinc and the risk of Parkinson's disease. *Neurotoxicology.* 1999;20(2–3):239–47.
- Zayed J, Ducic S, Campanella G, Panisset JC, Andre P, Masson H, et al. Environmental factors in the etiology of Parkinson's disease. *Can J Neurol Sci.* 1990;17(3):286–91.
- Hirsch EC, Brandel JP, Galle P, Javoy-Agid F, Agid Y. Iron and aluminum increase in the substantia nigra of patients with Parkinson's disease: an X-ray microanalysis. *J Neurochem.* 1991;56(2):446–51.
- Dexter DT, Carayon A, Javoy-Agid F, Agid Y, Wells FR, Daniel SE, et al. Alterations in the levels of iron, ferritin and other trace metals in Parkinson's disease and other neurodegenerative diseases affecting the basal ganglia. *Brain.* 1991;114(Pt 4):1953–75.
- Binolfi A, Rasia RM, Bertoncini CW, Ceolin M, Zweckstetter M, Griesinger C, et al. Interaction of alpha-synuclein with divalent metal ions reveals key differences: a link between structure, binding specificity and fibrillation enhancement. *J Am Chem Soc.* 2006;128(30):9893–901.
- Nielsen MS, Vorum H, Lindersson E, Jensen PH. Ca^{2+} binding to alpha-synuclein regulates ligand binding and oligomerization. *J Biol Chem.* 2001;276(25):22680–4.
- Lowe R, Pountney DL, Jensen PH, Gai WP, Voelcker NH. Calcium (II) selectively induces alpha-synuclein annular oligomers via interaction with the C-terminal domain. *Protein Sci.* 2004;13(12):3245–52.
- Moriarty GM, Minetti C, Remeta DP, Baum J. A Revised Picture of the Cu(II)-alpha-Synuclein Complex: The Role of N-Terminal Acetylation. *Biochemistry.* 2014;53(17):2815–7.
- Rasia RM, Bertoncini CW, Marsh D, Hoyer W, Cherny D, Zweckstetter M, et al. Structural characterization of copper(II) binding to α -synuclein: Insights into the bioinorganic chemistry of Parkinson's disease. *Proc Natl Acad Sci U S A.* 2005;102(12):4294–9.
- Uversky VN, Li J, Fink AL. Metal-triggered structural transformations, aggregation, and fibrillation of human alpha-synuclein. A possible molecular NK between Parkinson's disease and heavy metal exposure. *J Biol Chem.* 2001;276(47):44284–96.
- Wright JA, Brown DR. Alpha-synuclein and its role in metal binding: relevance to Parkinson's disease. *J Neurosci Res.* 2008;86(3):496–503.

34. Feng L, Xiao H, He X, Li Z, Li F, Liu N, et al. Long-term effects of lanthanum intake on the neurobehavioral development of the rat. *Neurotoxicol Teratol.* 2006;28(1):119–24.
35. Zhu W, Xu S, Shao P, Zhang H, Wu D, Yang W, et al. Bioelectrical activity of the central nervous system among populations in a rare earth element area. *Biol Trace Elem Res.* 1997;57(1):71–7.
36. Basu A, Chakrabarty K, Halder S, Addya S, Chatterjee GC. The effects of lanthanum chloride administration in newborn chicks on glutamate uptake and release by brain synaptosomes. *Toxicol Lett.* 1984;20(3):303–8.
37. Dobrynina N, Feofanova M, Gorelov I. Mixed lanthanide complexes in biology and medicine. *J Inorg Biochem.* 1997;67(1–4):168.
38. Pang X, Li D, Peng A. Application of rare-earth elements in the agriculture of China and its environmental behavior in soil. *Environ Sci Pollut Res Int.* 2002;9(2):143–8.
39. He ML, Wang YZ, Xu ZR, Chen ML, Rambeck WA. Effect of dietary rare earth elements on growth performance and blood parameters of rats. *J Anim Physiol Anim Nutr (Berl).* 2003;87(5–6):229–35.
40. Fricker SP. The therapeutic application of lanthanides. *Chem Soc Rev.* 2006;35(6):524–33.
41. Zhang J, Li Y, Hao X, Zhang Q, Yang K, Li L, et al. Recent progress in therapeutic and diagnostic applications of lanthanides. *Mini Rev Med Chem.* 2011;11(8):678–94.
42. Fernandez CO, Hoyer W, Zweckstetter M, Jares-Erijman EA, Subramaniam V, Griesinger C, et al. NMR of alpha-synuclein-polyamine complexes elucidates the mechanism and kinetics of induced aggregation. *EMBO J.* 2004;23(10):2039–46.
43. Koehler J, Meiler J. Expanding the utility of NMR restraints with paramagnetic compounds: Background and practical aspects. *Prog Nucl Magn Reson Spectrosc.* 2011;59(4):360–89.
44. Li C, Lutz EA, Slade KM, Ruf RA, Wang GF, Pielak GJ. 19 F NMR studies of alpha-synuclein conformation and fibrillation. *Biochemistry.* 2009;48(36):8578–84.
45. LeVine 3rd H. Quantification of beta-sheet amyloid fibril structures with thioflavin T. *Methods Enzymol.* 1999;309:274–84.
46. Khurana R, Coleman C, Ionescu-Zanetti C, Carter SA, Krishna V, Grover RK, et al. Mechanism of thioflavin T binding to amyloid fibrils. *J Struct Biol.* 2005;151(3):229–38.
47. Krebs MR, Bromley EH, Donald AM. The binding of thioflavin-T to amyloid fibrils: localisation and implications. *J Struct Biol.* 2005;149(1):30–7.
48. Pedersen JS, Dikov D, Flink JL, Hjuler HA, Christiansen G, Otzen DE. The changing face of glucagon fibrillation: structural polymorphism and conformational imprinting. *J Mol Biol.* 2006;355(3):501–23.
49. Conway KA, Lee SJ, Rochet JC, Ding TT, Williamson RE, Lansbury Jr PT. Acceleration of oligomerization, not fibrillization, is a shared property of both alpha-synuclein mutations linked to early-onset Parkinson's disease: implications for pathogenesis and therapy. *Proc Natl Acad Sci U S A.* 2000;97(2):571–6.
50. Hoyer W, Antony T, Cherny D, Heim G, Jovin TM, Subramaniam V. Dependence of alpha-synuclein aggregate morphology on solution conditions. *J Mol Biol.* 2002;322(2):383–93.
51. Garrett DS, Seok YJ, Peterkofsky A, Clore GM, Gronenborn AM. Identification by NMR of the binding surface for the histidine-containing phosphocarrier protein HPr on the N-terminal domain of enzyme I of the Escherichia coli phosphotransferase system. *Biochemistry.* 1997;36(15):4393–8.
52. Jones J, Wilkins D, Smith L, Dobson C. Characterisation of protein unfolding by NMR diffusion measurements. *J Biomol NMR.* 1997;10(2):199–203.
53. Rheinstetten G. TopSpin, version 2.1. Rheinstetten: Bruker BioSpin GmbH; 2007. p. Rheinstetten.
54. Delaglio F, Grzesiek S, Vuister GW, Zhu G, Pfeifer J, Bax A. NMRPipe: a multidimensional spectral processing system based on UNIX pipes. *J Biomol NMR.* 1995;6(3):277–93.
55. Goddard TD, Kneller DG. SPARKY 3. San Francisco: University of California; 2007.

Submit your next manuscript to BioMed Central and we will help you at every step:

- We accept pre-submission inquiries
- Our selector tool helps you to find the most relevant journal
- We provide round the clock customer support
- Convenient online submission
- Thorough peer review
- Inclusion in PubMed and all major indexing services
- Maximum visibility for your research

Submit your manuscript at
www.biomedcentral.com/submit

